Wireless Distributed Control with Open-Phase Fault-Tolerance for Delta-Connected Three-Phase Three-Wire Solid-State Transformers

Keita Ohata[1], Koki Yamanokuchi[1] and Jun-ichi Itoh[1]
[1] Nagaoka University of Technology, Japan

***Abstract*— This paper proposes wireless distributed control with a fault-tolerant for a solid-state transformer (SST) in single-wire open fault. A voltage imbalance occurs at the input side of each cell in the SST when an open-phase fault occurs. The voltage imbalance causes overmodulation in the power factor correction (PFC) converter. The proposed method employs the current droop control as an autonomous distributed control to achieve the voltage balance of each cell and prevent overmodulation without communication among each cell. The proposed method reduces the imbalance of the input voltage among series-connected cells by up to 95% compared to the control without the current droop control. Moreover, continuous operation is achieved during single-wire open-phase faults.**

***Index Terms*— Distributed control, Fault-tolerant, Solid-state transformer, Current droop control**

I. Introduction

Power distribution systems in the DC grid have been attracted to widespread renewable energies, such as photovoltaic systems. A solid-state transformer (SST) is the leading candidate for a replacement of a conventional AC-DC converter, which consists of a line-frequency transformer (LFT) and an AC-DC converter because the SST has various functions and advantages such as harmonic suppression, power flow control, and downsizing [1]-[7]. Generally, Input-Series-Output-Parallel (ISOP) configuration is used owing to a medium-voltage-AC (MVAC) and increasing the output power [1], [3]-[7]. The large-capacity SST consists of tens to hundreds of cells. Thus, many signal wires are required for centrally controlled SST. Moreover, if the centralized controller fails, the SST cannot continue operation [8]. Hence, the redundancy of the control configuration in the SST must be improved to introduce the SST as a part of the infrastructure equipment.

In order to improve the redundancy of the control configuration, a distributed control is applied. A typical distributed control scheme is a two-layer controller where the local controllers have a droop-based distributed controller, and the host controller has some additional compensators [9]-[10]. Some key element technologies have also been proposed to enhance the typical distributed control, such as the high synchronization accuracy technique [8], [11]-[13], cooperative control strategy with low-bandwidth communications [14]-[17]. However, adopting these enhanced controls is insufficient to deal with grid disturbances such as short circuits between line-to-line, ground faults, and imbalanced grid conditions. Some fault detection, localization, and tolerant controls are proposed [18]-[21]. However, these papers are targeted at the centralized control. The fault-tolerance control for grid disturbances in distributed controllers has not been well discussed. This paper focuses on single-wire open-phase faults in the distributed control.

Some open faults in the grid have been reported owing to the disconnection of transformer wiring [22]. The disconnection occurs by a strong wind or salty water. A continuous operation is possible as a single-phase converter using a two-wire connection when the single-wire open-phase fault occurs. Thus, the system should operate continuously as a single-phase converter in an emergency. In three-wire delta-connected SST, the part of the connection of cells changes to a series connection when the single-wire fault occurs. When the input current in each phase is controlled independently, control interference occurs among distributed controllers.

This paper proposes a distributed control with an open-phase fault-tolerant control method for a delta-connected three-phase three-wire SST with low-bandwidth wireless communication. The current droop control in the proposed method is adding a virtual admittance at the series-connected current source. The current droop control reduces the input voltage imbalance among series-connected cells. The new contribution of this paper is achieving continuous operation without overmodulation during open-phase faults in distributed controlled SSTs. Furthermore, the voltage stress on switching devices is equalized. Therefore, it is expected to achieve easy system management when an open-phase fault occurs. As a second benefit, the proposed method does not require high-speed wired communication.

This paper is organized as follows; first, the circuit configuration of the proposed circuit and the proposed distributed control scheme is described; next, the fundamental characteristics of the current droop control are shown; moreover, the current droop parameter is designed for the single open-phase fault-tolerant operation; at last, the proposed method is verified by the 7.2-kW six-cell prototype.

II. Circuit Configuration

Figure 1 shows the proposed three-phase three-wire SST with low-bandwidth wireless distributed control. The SST is connected to a three-phase MVAC. A diode bridge

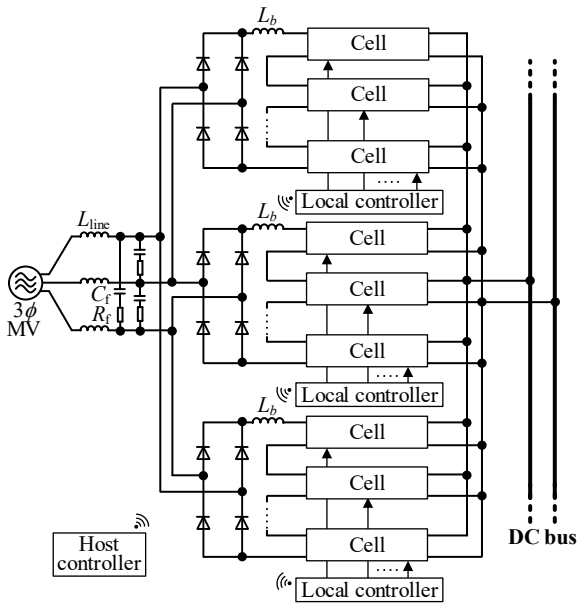

Fig. 1: Proposed three-phase three-wire solid-state transformers.

is connected to the input of each phase, and small-capacity converters (cells) are connected in series at the rear of the diode bridge. The outputs of the cell converters are connected to the DC bus in parallel.

Figure 2 shows the circuit diagram of the cell converter. The cell converter consists of a PFC converter and a resonant DC-DC converter. The resonant DC-DC converter utilizes the resonance between L_s and C_s in order to perform soft switching. In the system, the resonant DC-DC converter is driven at a constant switching frequency without the output voltage control. As a result, the resonant DC-DC converter performs a DC-DC transformer with a constant voltage transfer ratio. Thus, the output power from each phase fluctuates at twice the frequency of the grid frequency. However, the fluctuation of the output power from each phase has 120 degrees of phase differences among other phase cells. Hence the sum of the output power of the system is constant without any control in the DC-DC converter. In other words, the DC-link capacitors on the primary and secondary sides do not need to compensate for the fluctuation. For this reason, the small capacitance of the DC link capacitor and the output capacitor is accepted.

III. Proposed Control Scheme

Figure 3 shows the proposed control block diagram. The controller of this system consists of a two-layer structure: a host controller and local controllers. The host controller transmits the input current command I_{in}^* to each local controller. The host controller also receives the status of the cell converters from each local controller. The local controller controls the input current i_{in} based on the received command from the host controller through wireless communication. The series-connected cells in each phase are driven by phase-shifted carriers, contributing to L_b miniaturization.

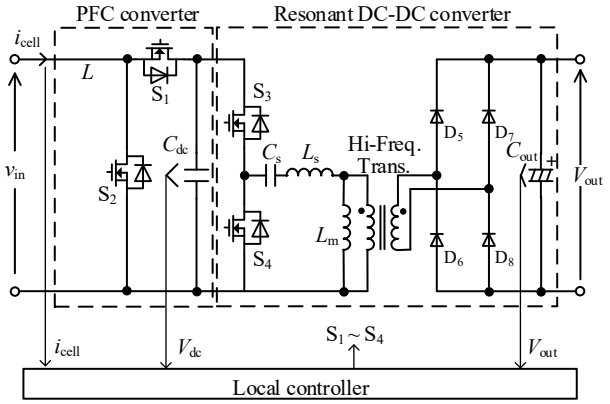

Fig. 2: Configuration of cell converters.

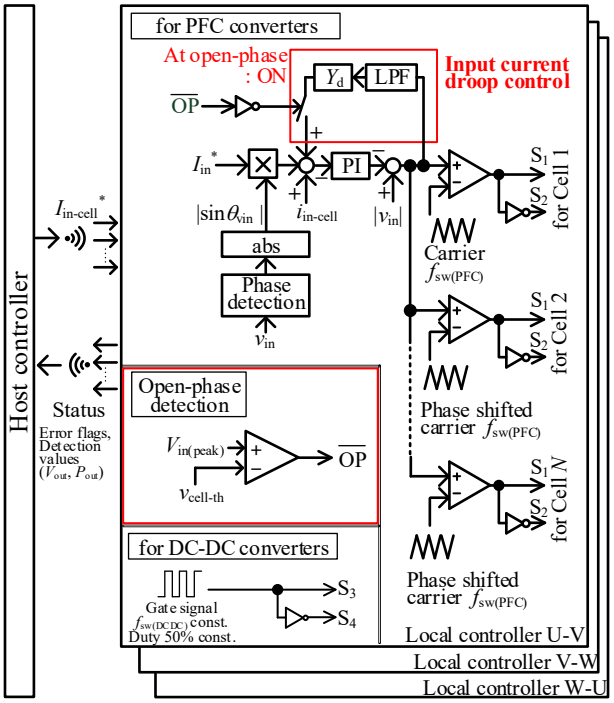

Fig. 3 Proposed signal wireless distributed controller.

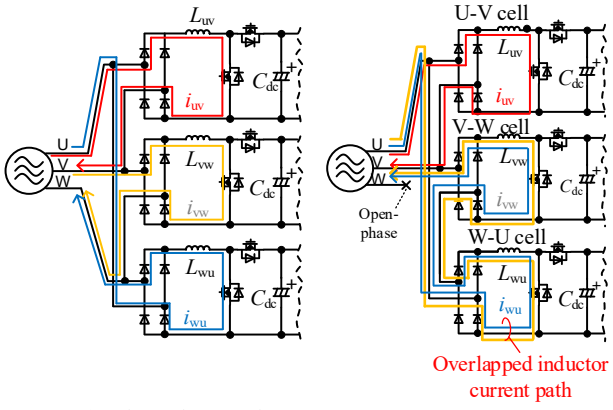

(a) Three-phase mode. (b) W-phase open-phase mode.

Fig. 4. Current path of grid current.

A. Three-phase mode

Figure 4(a) shows the current path in a three-phase operation. During three-phase, no control interference

occurs for current control because the current path of each inductor is controlled independently.

B. Single-wire open-phase mode

Figure 4(b) shows the current path when the W-phase opens. The V-W and W-U cells are connected in series between U and V-phases. In other words, inductors L_{vw} and L_{wu} are connected in series. Local controllers control inductor currents, respectively. Thus, interference among current controllers occurs, as shown in Fig. 5(a). This paper proposes open-phase fault-tolerant control by the current droop control in order to prevent control interference.

Figure 5(b) shows the equivalent circuit when the current droop is implemented. The input current of each cell is controlled by local controllers. Hence, the cell is equivalent to a current source. Note that the series-connected cells in each phase drive the same inductor L_b using the phase-shifted carrier. Thus the equivalent circuit is also the same when the number of cells increases. When the current sources output different currents, control interference occurs because the operation conflicts with Kirchhoff's current law.

The current droop control is implemented to solve this problem. The droop control in this context means the addition of virtual admittance in parallel with these current sources. The current droop control is the duality relation between the well-known droop control for parallel connected power converters [9]-[10]. The interference among the current controllers is suppressed by the virtual current in the virtual admittance.

IV. Characteristic of Current Droop Controller

In this section, the characteristics of the current droop control are mentioned. This paper focuses on the voltage and the current of each cell.

A. Current deviation

When the current droop control is applied during a W-phase open fault, the grid current i_{grid} is given by (1) from Fig 5 (b), which is applied to the principle of superposition.

$$i_{grid} = \frac{3}{2} Y_d v_g + i_{uv} + \frac{i_{vw}}{2} + \frac{i_{wu}}{2} \tag{1}$$

where Y_d is virtual admittance, v_g is grid voltage, and i_{uv}, i_{vw}, i_{wu} are the actuating value of the input current controller in each local controller. When i_{uv}, i_{vw}, and i_{wu} have the detection errors ε_{iuv}, ε_{ivw}, and ε_{iwu}, respectively, each cell current i_x is controlled to,

$$i_x = (1-\varepsilon_{ix}) i_{in}^{*} \quad (x\text{=uv, vw or wu}) \tag{2},$$

where i_{in}^{*} is the input current command. Thus, (1) with detection error of current is rearranged to

$$i_{grid} = \frac{3}{2} Y_d v_g + (1-\varepsilon_{iuv}) i_{in}^{*} + \frac{(1-\varepsilon_{ivw}) i_{in}^{*}}{2} + \frac{(1-\varepsilon_{iwu}) i_{in}^{*}}{2} \tag{3}.$$

the input current i_{in} at the series connected cells, VW-cell and WU-cell, is given by,

$$i_{in} = \frac{1}{2} Y_d v_g + \frac{(1+\varepsilon_{ivw}) i_{in}^{*}}{2} + \frac{(1+\varepsilon_{iwu}) i_{in}^{*}}{2} \tag{4}.$$

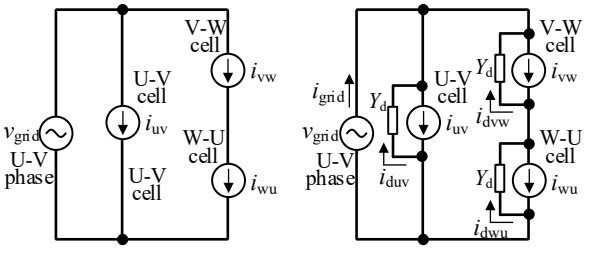

(a) without current droop control. (b) with current droop control.

Fig. 5 Equivalent circuit on the AC grid side at open W phase (in the case of Fig.4(b)).

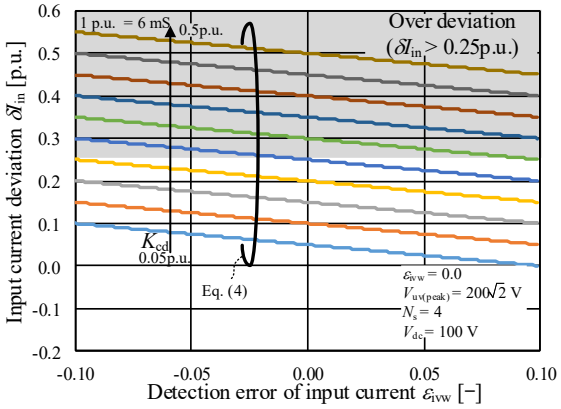

Fig. 6 Current deviation characteristics when the current droop gain and the detection error of input current are changed.

Figure 6 shows the input current deviation δI_{in}. The deviation is calculated from (4). The input current detection ε_{ivw} is changed from -10% to +10%, and the current droop gain K_{cd} is changed from 0.05p.u. to 1.0p.u.. the DC bus voltage is set to 80 V. the current droop gain K_{cd} and the input current deviation δI_{in} are defined as:

$$K_{cd} = \frac{Y_d}{Y_{load}} \tag{5},$$

$$\delta I_{in} = \frac{I_{in} - I_{in}^{*}}{I_{in}^{*}} \tag{6},$$

where I_{in}^{*} is the current command. Note that the winding ratio of the transformer in the resonant DC-DC converter N_{sec}/N_{pri} is set to 2.0, and the DC-DC converter is driven with constant frequency. As a result, the DC-link voltage V_{dc} and the output voltage V_{out} always maintain a constant ratio of 1:1 in the configuration. The input current deviation δI_{in} increases with the detection error of the input current at VW-cell ε_{ivw}. Moreover, the deviation δI_{in} increases with increasing the current droop gain K_{cd}. Thus, the current droop gain K_{cd} should be as small as possible to suppress the current deviation. The maximum gain of current droop control is determined by the specification of the allowable current deviation. For example, the maximum current deviation is specified as 25% of the

command value, and an input current detection error of ±10% is tolerated when K_{cd} is 0.4 p.u. or less.

B. Input voltage Imbalance

The sums of input voltages of each phase series-connected cell $V_{vwcells(peak)}$ and $V_{wucells(peak)}$ are given by (7) and (8) from Fig. 5 (b) when the current droop control is applied during a W-phase open fault,

$$V_{vwcells(peak)} = \frac{1}{2Y_d} i_{in}^* \left\{ (1+\varepsilon_{ivw}) - (1+\varepsilon_{iwu}) \right\} + \frac{1}{2} V_{uv} \quad (7)$$

$$V_{wucells(peak)} = \frac{1}{2Y_d} i_{in}^* \left\{ (1+\varepsilon_{iwu}) - (1+\varepsilon_{ivw}) \right\} + \frac{1}{2} V_{uv} \quad (8)$$

Figure 7 shows the peak value of the input voltage calculated from (7) and (8). the input current detection ε_{ivw} is changed from -10% to +10%, and the current droop gain K_{cd} is changed from 0.1p.u. to 0.5p.u.. when the VW- local controller detects the input current with a negative detection error, the VW-controller tries to increase the input current compared to the WU-controller. Hence, the $V_{vwcells(peak)}$ increase and $V_{wucells(peak)}$ decrease. In addition, when K_{cd} is increased, the increasing detection error is smaller. Thus, the current droop gain K_{cd} should be as large as possible to suppress the input voltage imbalance between series-connected cells VW-cells and WU-cells. The non-overmodulation condition determines the minimum current droop gain. The condition is obtained from the peak input voltage of each cell $V_{in(peak)}$ and the DC link voltage V_{dc}. The non-overmodulation condition is expressed by,

$$V_{in(peak)} < V_{dc} \quad (9).$$

Note that the $V_{in(peak)}$ is given by,

$$V_{in(peak)} = \frac{\sqrt{2} V_{grid}}{2N_s} \quad (10),$$

where N_s is the number of series-connected cells in each cell, and V_{grid} is the root mean square value of the grid voltage between line-to-line. For example, N_s and V_{out} are specified as 2 and 100 V, respectively. Then the minimum K_{cd} must be at 0.14p.u. or more.

V. Design of Current Droop Gain for Open-Phase Fault-Tolerant Control

This section shows the design of the current droop gain K_{cd} for the open-phase fault-tolerant operation based on Section III. The design has been enhanced based on [23]-[24] to apply the open-phase failure. The stability of the current droop control is decreased by the computation delay and the PWM delay due to the digital control. The effect has already been discussed in [24]. As a result, the current droop control is stable in the region, which is sufficiently lower than the current control bandwidth. In this paper, the stable region is used. Hence, this paper focuses on the design of the current droop gain for open-phase fault-tolerant control.

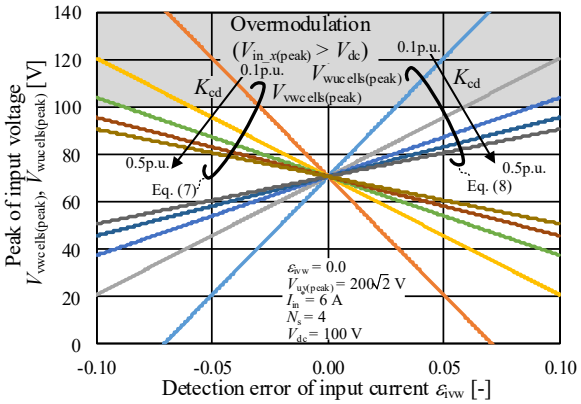

Fig. 7. Input voltage characteristics of each series connected cell when the current droop gain and the detection error of input current are changed.

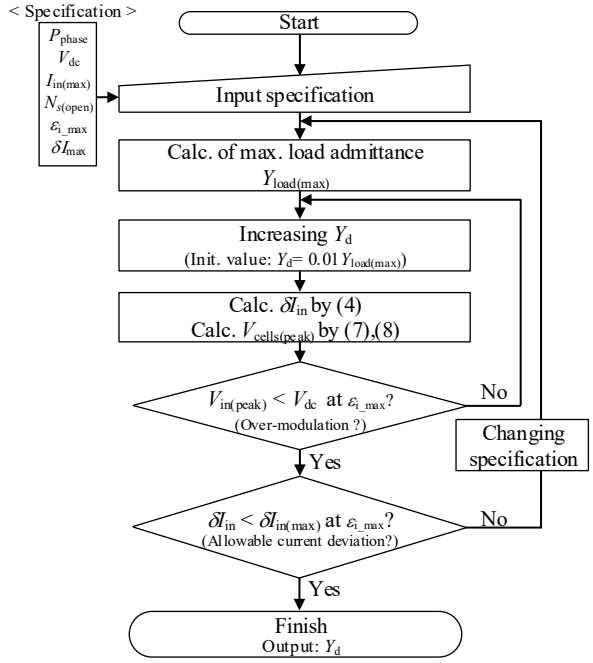

Fig.8. Design flowchart of current droop admittance Y_d.

Figure 8 shows the design flowchart of the current droop gain K_{cd}. The design requires the six specifications of the SST as follows:

1) Rated power of cell P_{cell}
2) DC-link voltage V_{dc}
3) Maximum input current $I_{in(max)}$
4) Number of series-connected cells during single-wire open-phase fault $N_{s(open)}$
5) Allowable input current deviation δI_{max}
6) Allowable detection error of input current ε_{imax}

First, the maximum input admittance $Y_{in\_phase(max)}$ of the SST is calculated from the specifications. Second, the gain K_d is set to $0.01 Y_{in\_phase(max)}$ at the first time. Third, (4) calculates to derive the input current deviation δI_{in}. In addition, (7) and (8) calculate to derive the sums of input voltages of each phase series-connected cell $V_{vwcells(peak)}$ and $V_{wucells(peak)}$. Fourth, checking that the condition is non-overmodulated. When the condition is satisfied, the current droop gain K_{cd} should be increased again. The trial

is repeated to obtain the minimum current droop gain K_{cd} without over-modulation. Depending on the specification of δI_{max} and ε_{imax}, the overmodulation and the current deviation may not be satisfied at the same time. Then, the changing specification is required. Note that when a voltage controller is added to the outer current controller, the voltage controller compensates for the current deviation. Then, there is no problem with the current deviation. However, the additional output voltage droop controller is needed to prevent voltage control interference among parallel connected cells [15].

Figure 9 shows the operation area. The input current deviation and the detection error of input current limit the area. In Section VI, The gain design is verified at two operation points, *A* (Overmodulation) and *B* (Desirable operation).

Table I lists the design specification and the derived value of the current droop gain K_{cd}. K_{cd} is set to 0.05p.u. or 0.2 p.u. The designed gain is used in Section VI.

VI. Experimental Results

Fig. 10 shows the experimental environment. A delta-connected prototype SST consists of two cells in each phase. Three local controllers independently control each cell. The SST is connected to the three-phase three-wire grid. An RC filter is provided at the input of the SST to remove switching frequency components in the input current. The single-wire open-phase fault is emulated by opening the magnet contactor. The open-phase fault is automatically detected from a decrease in the input voltage.

A. Steady response during single-wire open-phase fault

Figure 11(a) shows the input voltage of each cell and input current when the current droop control is not applied. The modulation rate of VW-cells m_{vw} is over 1.0. Thus, The input current cannot be controlled sinusoidally.

Figure 11(b) shows the waveform when the current droop control is applied with K_{cd}=0.05p.u. (Y_{cd}=3mS). The input voltage imbalance is 200 V, and overmodulation occurs. Thus, the gain is not sufficient.

Figure 11(c) shows the waveform when the current droop control is applied with K_{cd}=0.2p.u. (Y_{cd}=12mS). The input voltage imbalance is 40 V. Thus, the imbalance is reduced by 80% compared to Fig.11(b) condition.

Figure 12 shows the transient response from three-phase to single-wire open-phase fault during W-phase open fault. The input voltage imbalance between series-connected cells $v_{in(VW\text{-}cell)}$ and $v_{in(WU\text{-}cell)}$ is suppressed for about three cycles. Note that a surge voltage occurs at the SST input due to the wiring inductance from the open fault point to the SST input. On the other hand, an absorber is generally installed to suppress the lightning surge voltage. Thus, the surge voltage due to the open-phase fault is not applied directly to the switching device.

B. Transient response from single-wire open-phase fault to Three-phase mode

Figure 12 shows the transient response from the three-phase mode to the open-phase fault-tolerant mode. Each local controller automatically changes the operation mode

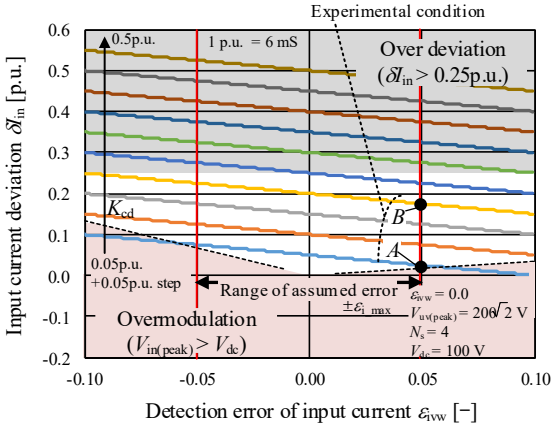

Fig.9 Allowable operation area. The operation area is limited by the input current deviation characteristics and the design flowchart of current droop gain.

TABLE I
Design Specifications and Experimental Conditions

Name	Symbol	Value
Input voltage	V_{in}	200 Vrms
Number of series connected cells at single-wire open-phase fault	N_s	4
Output power	P	7.2 kW (1.2 kW × 6 cells)
Output voltage	V_{out}	100 V (Fig. 11) 150 V (Fig. 12, 13)
Wiring ratio of transformer	N_1/ N_2	1:2 (V_{out} = V_{dc})
Boost inductance	L_b	3 mH (%Z=2.8 %)
DC-link capacitance	C_{conv}	1080 μF (H = 35 ms)
Resonant inductor	L_s	10 μH
Resonant capacitor	C_s	0.45 μF
Output capacitance	C_{out}	1080 μF (H = 35 ms)
Resonant frequency	f_{res}	75 kHz
Switching freq. at PFC	$f_{sw(PFC)}$	45 kHz
Switching freq. at res. DC-DC	$f_{sw(DC\text{-}DC)}$	85 kHz
Maximum input admittance	$Y_{load(max)}$	60 mS
Detection error of input current	ε_{ivw}	+5%
	ε_{iwu}	0%
Current droop admittance	Y_{cd}	3 mS (*A* in Fig. 9) 12 mS (*B* in Fig. 9)
Current droop gain	K_{cd}	0.05 p.u. (*A* in Fig. 9) 0.2 p.u. (*B* in Fig. 9)

H: Unit capacitance constant of output capacitance based on converter capacity

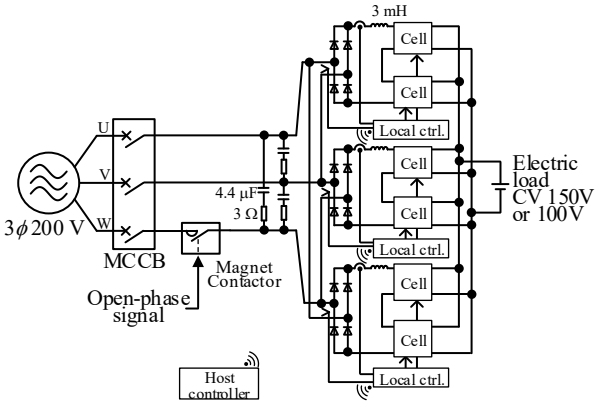

Fig. 10 Experimental environment. The SST is connected to a Three-phase 3-wire grid. Each local controller outputs PWM signals using phase-shifted carriers for series-connected cells.

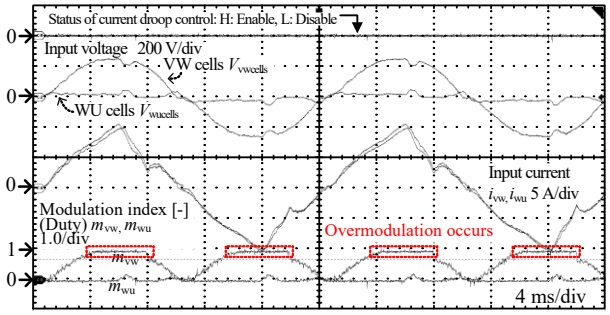

(a) Without current droop control.

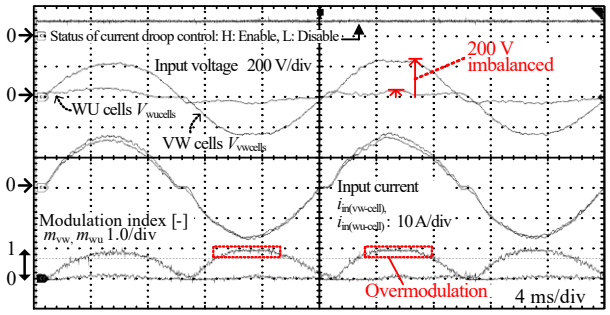

(b) With current droop control K_{cd}=0.05p.u.(Y_d=3 mS) (at *A* in Fig. 9).

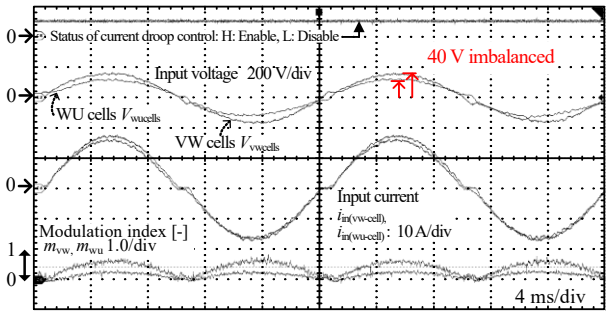

(c) With current droop control K_{cd}=0.2p.u.(Y_d=12 mS) (at *B* in Fig.9).

Fig.11 Input voltage and input current at steady state during W-phase open fault. ε_{vw} is 0.05 (+5%), ε_{wu} is 0 (+0%).

to the fault-tolerant operation without communication among cells.

Figure 13 shows that the single-wire open-phase fault is removed, and the sum of input voltages of each phase series-connected cell is recovered to 200 V. Each slave controller detects the recovered voltage, and the SST is restored from the fault mode to the three-phase mode quickly without the signal communication among local controllers. After returning to the three-phase operation, the input voltage and the input current are controlled to the same phase as the input voltage in 20 ms, and the three-phase function is restored.

VII. Conclusion

This paper proposed a single-wire open-phase fault-tolerant method for a delta-connected three-phase three-wire SST. The current droop control was employed to prevent the current control interference. The proposed method prevented overmodulation due to the input voltage

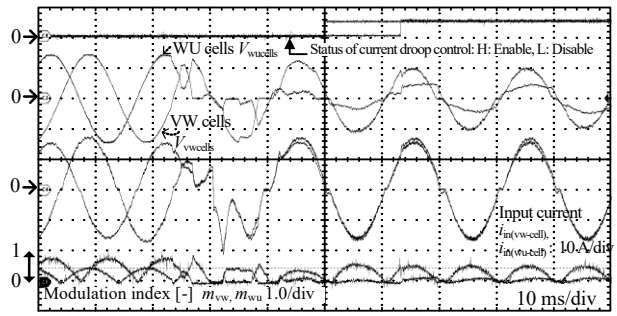

Fig. 12 Transient response from three-phase to W-phase open fault-tolerant. ε_{vw} is 0.05 (+5%), ε_{wu} is 0 (+0%).

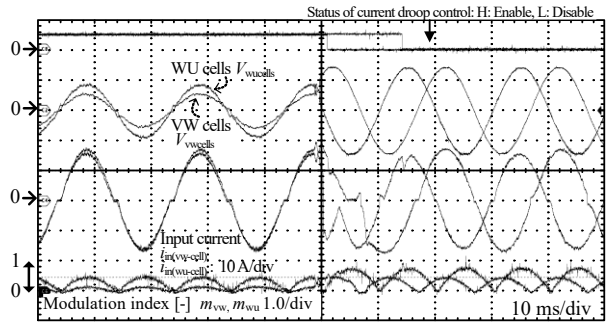

Fig. 13 Transient response from W-phase open fault to three-phase operation. ε_{vw} is 0.05 (+5%), ε_{wu} is 0 (+0%).

imbalance among series-connected cells. The proposed current droop method reduced the voltage imbalance by up to 95% compared to the case without the current droop control.

In future work, the local controller will be installed in each cell, not in each phase, in order to improve the redundancy.

References

[1] H. Fan and H. Li, "High-Frequency Transformer Isolated Bidirectional DC–DC Converter Modules With High Efficiency Over Wide Load Range for 20 kVA Solid-State Transformer," *IEEE Trans. Power Electron.*, vol. 26, no. 12, pp. 3599–3608, Dec. 2011

[2] G. Ortiz, M. G. Leibl, J. E. Huber, and J. W. Kolar, "Design and Experimental Testing of a Resonant DC–DC Converter for Solid-State Transformers," *IEEE Trans. Power Electron.*, vol. 32, no. 10, pp. 7534–7542, Oct. 2017.

[3] J. Itoh, K. Aoyagi, K. Kusaka, and M. Adachi, "Development of Solid-state Transformer for 6.6-kV Single-phase Grid with Automatically Balanced Capacitor Voltage," *IEEJ Journal IA*, vol. 8, no. 5, pp. 795–802, Sep. 2019.

[4] M. Nakahara, Y. Kawaguchi, K. Furukawa, M. Kadota, Y. Mabuchi, and A. Kanoda, "Development of a Control Method for LLC Converter Utilized for Input-Parallel-Output-Series Inverter System with Solid-State Transformers," *IEEJ Journal IA*, vol. 8, no. 4, pp. 652–659, Jul. 2019

[5] J. Chen, T. Yang, C. O'Loughlin, and T. O'Donnell, "Neutral Current Minimization Control for Solid State Transformers Under Unbalanced Loads in Distribution Systems," *IEEE Trans. Ind. Electron.*, vol. 66, no. 10, pp. 8253–8262, Oct. 2019

[6] J. Chen, T. Yang, C. O'Loughlin, and T. O'Donnell, "Neutral Current Minimization Control for Solid State

Transformers Under Unbalanced Loads in Distribution Systems," *IEEE Trans. Ind. Electron.*, vol. 66, no. 10, pp. 8253–8262, Oct. 2019

[7] Y. Kawai, K. Izumi, and H. Haga, "A Phase-Shift Control Method of Triple-Active-Bridge Converter for Reducing Power Loss Under Light Load Condition", *IEEJ Journal IA*, vol. 12, pp. 162-175, 2023.

[8] M. A. Parker, L. Ran, and S. J. Finney, "Distributed Control of a Fault-Tolerant Modular Multilevel Inverter for Direct-Drive Wind Turbine Grid Interfacing," *IEEE Trans. Ind. Electron.*, vol. 60, no. 2, pp. 509–522, Feb. 2013

[9] J. M. Guerrero, P. C. Loh, T.-L. Lee, and M. Chandorkar, "Advanced Control Architectures for Intelligent Microgrids—Part II: Power Quality, Energy Storage, and AC/DC Microgrids," *IEEE Trans. Ind. Electron.*, vol. 60, no. 4, pp. 1263–1270, Apr. 2013

[10] S. Anand, B. G. Fernandes, and J. Guerrero, "Distributed Control to Ensure Proportional Load Sharing and Improve Voltage Regulation in Low-Voltage DC Microgrids," *IEEE Trans. Power Electron.*, vol. 28, no. 4, pp. 1900–1913, Apr. 2013

[11] C. L. Toh and L. E. Norum, "Implementation of high speed control network with fail-safe control and communication cable redundancy in modular multilevel converter," in *Proc. 2013 15th European Conference on Power Electronics and Applications*, Lille, France, Sep. 2013, pp. 1–10.

[12] S. Rietmann, S. Fuchs, A. Hillers, and J. Biela, "Field Bus for Data Exchange and Control of Modular Power Electronic Systems with High Synchronisation Accuracy of ±4 ns," *IEEJ Journal IA*, vol. 8, no. 2, pp. 295–305, Mar. 2019

[13] Y. Rong et al., "A Synchronous Distributed Communication and Control System for SiC-Based Modular Impedance Measurement Units," *IEEE J. Emerg. Sel. Topics Power Electron.*, vol. 10, no. 3, pp. 3182–3194, Jun. 2022

[14] X. Lu, J. M. Guerrero, K. Sun, and J. C. Vasquez, "An Improved Droop Control Method for DC Microgrids Based on Low Bandwidth Communication With DC Bus Voltage Restoration and Enhanced Current Sharing Accuracy," *IEEE Trans. Power Electron.*, vol. 29, no. 4, pp. 1800–1812, Apr. 2014

[15] K. Ohata et al., "Decentralized Control Using Wireless Signal Communication for Solid-state Transformer with Cascaded Chopper Cell," in *Proc. 2020 IEEE 9th Int. Power Electron. and Motion Control Conf.*, Nanjing, China, Nov. 2020, pp. 531–537

[16] B. Çiftçi, S. Schiessl, J. Gross, L. Harnefors, S. Norrga, and H.-P. Nee, "Wireless Control of Modular Multilevel Converter Submodules," *IEEE Trans. Power Electron*., vol. 36, no. 7, pp. 8439–8453, 2021

[17] M. Sakamoto and H. Haga, "Control Method for Single-Phase Active Filter Using Universal Smart Power Module (USPM)," *IEEJ Journal IA*, Article ID: 22006895, Dec. 2022

[18] P. Lezana, J. Pou, T. A. Meynard, J. Rodriguez, S. Ceballos, and F. Richardeau, "Survey on Fault Operation on Multilevel Inverters," *IEEE Trans. Ind. Electron.*, vol. 57, no. 7, pp. 2207–2218, Jul. 2010

[19] F. Deng, Z. Chen, M. R. Khan and R. Zhu, "Fault Detection and Localization Method for Modular Multilevel Converters", *IEEE Trans. Power Electron.*, vol. 30, no. 5, pp. 2721-2732, 2015

[20] N. B. Y. Gorla, S. Kolluri, M. Chai and S. K. Panda, "A Novel Open-Circuit Fault Detection and Localization Scheme for Cascaded H-Bridge Stage of a Three-Stage Solid-State Transformer", *IEEE Trans. on Power Electron.*, vol. 36, no. 8, pp. 8713-8729, 2021

[21] J. Han, Z. Zhang, Q. Lai and X. Yin, "Open-Circuit Fault Characteristics and Location Methods of Switch Elements For Cascaded Power Electronic Transformers," *IEEE Trans. on Power Delivery*, vol. 37, no. 2, pp. 1017-1026, 2022

[22] Investigating R&D Committee on Aging Management of Distribution Equipment, "Investigation and Technical Trends to Deal with Aging Management of Distribution Equipment", Japan, *IEEJ Technical Report*, No. 1469, 2019 (in Japanese)

[23] K. Yamanokuchi, H. Watanabe, and J.-I. Itoh, "Droop-based Current Control Method in Autonomous Distributed Modular Power Conversion System," in *Proc. 2021 IEEE Applied Power Electron. Conf. and Expo.*, Phoenix, AZ, USA, Jun. 2021, pp. 660–667.

[24] K. Yamanokuchi, H. Watanabe, and J.-I. Itoh, "Comparison of Controllers with Current Droop Capability for Series-Connected Autonomous Distributed Modular Power Converter", in *Proc. 2022 IEEE Applied Power Electron. Conf. and Expo.*, Houston, TX, USA, Mar. 2022, pp. 777-784.